

## Direct Observation of a Defect-Mediated Viscoelastic Transition in a Hydrogel of Lipid Membranes and Polymer Lipids

S. L. Keller,<sup>1,\*</sup> H. E. Warriner,<sup>2,†</sup> C. R. Safinya,<sup>2,‡</sup> and J. A. Zasadzinski<sup>1,§</sup>

<sup>1</sup>Materials and Chemical Engineering Departments, University of California, Santa Barbara, California 93106

<sup>2</sup>Materials Department, Physics Department, Bioc. and Mol. Biology Program, University of California, Santa Barbara, California 93106

(Received 20 January 1997)

We present the first direct imaging of a new hydrogel of lipid membranes containing polymer lipids. Freeze-fracture electron microscopy shows unambiguously that the hydrogel's surprisingly large viscoelasticity is explained by a novel defect topology of *interconnections* between defects. The defects are spherulites with high membrane curvatures which are either isotropic or cylinderlike. A lower concentration of dislocation-type defects was also observed. The interconnections between the defects distinguish the hydrogel from simple "onion" phases of multilamellar vesicles with a smaller viscoelasticity. [S0031-9007(97)03388-7]

PACS numbers: 61.72.Ff, 61.16.Bg, 68.10.Et

Polymer hydrogels constitute an important class of "soft" materials with uses as implants and tissue replacements, drug delivery systems, and bioseparation media [1,2]. In particular, materials based upon lipids and polyethylene glycol (PEG) have biomedical applications due to low immunogenicity (e.g., "stealth liposomes") [1,3,4]. When PEG polymers are covalently attached to lipids, PEG-lipids are created.

A new system with potential applications (tissue healing, drug delivery, or cosmetics applications) is the PEG-lipid "lamellar hydrogel  $L_{\alpha,g}$ ." Warriner *et al.* recently used x-ray diffraction, polarized light microscopy, and rheometry to study this new hydrogel composed of multiple layers of surfactant membranes and small amounts of a polymer lipid (Fig. 1) [5]. The hydrogel possesses a surprisingly high viscoelasticity, higher than that of multilamellar vesicle phases (MLVs or "onions," concentric shells of lipid membranes). The hydrogel also differs from "onion" phases in that it remains a single-phase gel at high water dilution (90%) and becomes *more* viscoelastic upon dilution. Using freeze-fracture electron microscopy and polarized optical microscopy, we show that the hydrogel's high viscosity is linked to a proliferation of membrane defects interconnected by bilayer sheets. The liquid-to-gel phase transition is driven by mesoscopic topological defects rather than by changing molecular properties.

X-ray diffraction of the hydrogel found that the lipids' hydrocarbon chains remain liquidlike in both the liquid and gel phases (Fig. 1). Thus, the addition of a PEG-lipid does not affect bilayer fluidity, and, unlike  $L_{\beta'}$  gels, gelation is not due to in-plane ordering of the lipids [5]. PEG-lipid molecules diffuse freely in the plane of the membrane. Bilayers in this study are constructed of 4:1 pentanol:lipid, where the lipid is dimyristoylphosphatidylcholine (DMPC) and PEG-lipid. Pentanol reduces the bending rigidity of the lipid membranes ( $\kappa \approx k_B T$ ) and increases thermal membrane undulations [7]. The PEG-

lipid's PEG head has a molecular weight of 2053 g/mol and its lipid base is dimyristoylphosphatidylethanolamine (DMPE). The addition of a PEG-lipid to flexible lipid bilayers creates a hydrogel.

An unusual aspect of the hydrogel is an *increase* in viscoelasticity upon dilution with water, opposite the behavior of gels of isotropically dispersed polymer

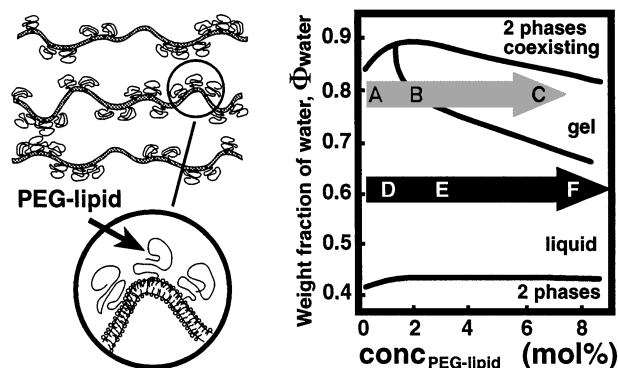


FIG. 1. Left: schematic of fluid membranes with polymer lipids. Right: phase diagram redrawn from Warriner *et al.* [5]. The weight fraction of water,  $\Phi_{\text{water}}$ , is plotted vs  $\text{conc}_{\text{PEG-lipid}} = c_{\text{PEG}} = 100 \times (\text{number PEG-lipid molecules}) / (\text{total number lipid molecules})$ . The sample is biphasic (lamellae and excess water) only at very high water concentrations. In contrast, gels of frozen-chain  $L_{\beta'}$  phase bilayers have an excess water phase at  $>40\%$  water [6]. At low water fractions ( $\Phi_{\text{water}} \leq 45\%$ ), membranes are separated by  $d_{\text{water}} \approx 25 \text{ \AA}$  which is too small to incorporate a swollen PEG polymer, and the system separates into two phases, lamellar and isotropic [5]. The hydrogel is reached from the liquid phase by dilution or by addition of PEG-lipid. Samples A, B, C, D, E, and F were investigated by freeze-fracture electron microscopy and polarized optical microscopy. Sample A contained  $\Phi_{\text{water}} = 80\%$  and  $c_{\text{PEG}} = 0.3\%$ ; sample B:  $\Phi_{\text{water}} = 77\%$  and  $c_{\text{PEG}} = 4.19\%$ ; sample C:  $\Phi_{\text{water}} = 81\%$  and  $c_{\text{PEG}} = 7.7\%$ ; sample D:  $\Phi_{\text{water}} = 64\%$  and  $c_{\text{PEG}} = 1.15\%$ ; sample E:  $\Phi_{\text{water}} = 64\%$  and  $c_{\text{PEG}} = 3.05\%$ ; and sample F:  $\Phi_{\text{water}} = 60\%$  and  $c_{\text{PEG}} = 8.1\%$ .

networks. Defects inhibit flow and lead to gelation. To elucidate the mechanism of gelation and the defect structure on length scales from  $\sim 10$  nm to 1 mm, we combined freeze-fracture electron microscopy and polarized optical microscopy. Freeze fracture was performed as in Chiruvolu *et al.* [8] and the replicas processed as in Fetter and Costello [9], except that they were bathed in ethanol and retrieved on formvar-coated microscopy grids. Replicas were imaged in a transmission electron microscope JEOL100CX at an accelerating voltage of 100 keV.

As PEG-lipid concentration increased across the liquid-to-gel transition (gray arrow, Fig. 1), domain sizes of lamellar regions decreased. Membrane bilayers became more curved and organized into defects interconnected by additional bilayers (Fig. 2). By electron microscopy, sample *A* (Fig. 1) in the liquid, low-viscosity phase exhibited predominantly well-ordered, gently curving lamellae seen edge on at the star in Fig. 2(a). In places without defects, the micrograph was filled with long, parallel sheets of membranes, spanning microns. Lamellae were occasionally interspersed with spherulite defects [Fig. 2(a), arrows]. Spherulites are essentially multilamellar vesicles (or type-II focal conics with the defining hyperbola reduced to a line and the ellipse reduced to a point [10]). Spherulites were typically  $\sim 1$   $\mu\text{m}$  and were occasionally ellipsoidal and anisotropic or showed the rugby-ball ends of a general type-II focal conic. The spherulites themselves are thermodynamically stable. Lamellae with-

out defects were rare, which is not surprising since the samples were not annealed [11].

At the transition from the low-viscosity liquid to the high-viscosity gel, sample *B* (Fig. 1) had a higher defect density than the fluid sample *A*. Regions of smaller, high-curvature spherulite defects  $\sim 0.5$   $\mu\text{m}$  [Fig. 2(b), arrow] were embedded in lamellae so that they were connected by a network of bilayer sheets. When the fracture followed a connecting sheet, the spherulite structure below was visible [Fig. 2(b), star]. Thick, planar stacks of lamellar bilayers were less common in this transition sample than in the fluid.

Deep within the viscous gel phase, sample *C* (Fig. 1) had a high defect density. The most common morphology was polydisperse,  $\sim 0.2$   $\mu\text{m}$  spherulites (both isotropic and anisotropic) connected by additional membranes and filling all volume [Fig. 2(c), arrow]. Spherulites were often distorted by tightly packed neighbors or their interior layers were bent into crescents [Fig. 2(c), stars]. Although nearly cylindrical and anisotropic spherulites were common; large and well-aligned ones were uncommon. Some appear in Fig. 3(a) (stars) among smaller spherulites (black arrow) and connecting bilayers (white arrow). Well-ordered or undulating lamellae [Fig. 3(b), stars] were rare. Some lamellar regions ended in disclination defects [Fig. 3(b), arrow].

The origin of the hydrogel's high viscoelasticity is revealed directly by the electron micrographs above. First,

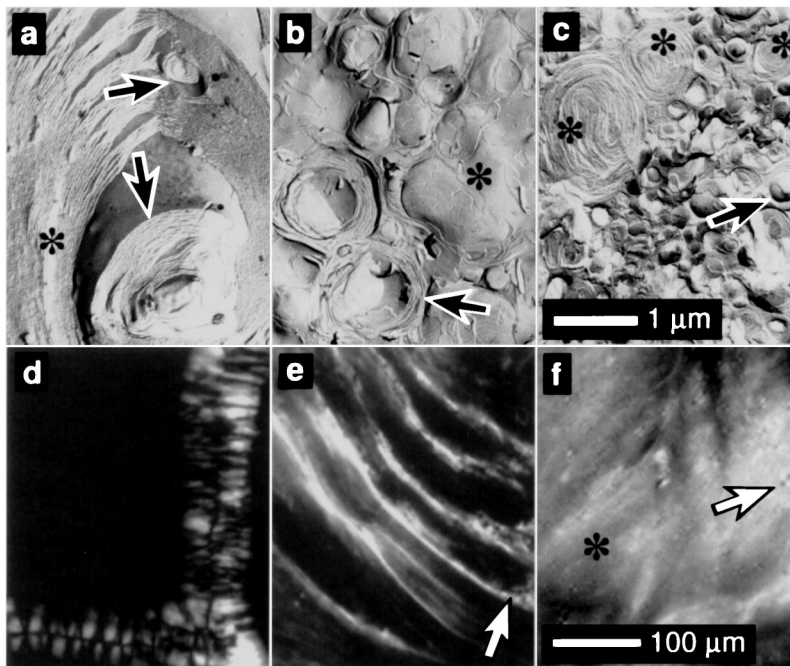


FIG. 2. Samples crossing the liquid to hydrogel transition (Fig. 1, gray arrow) appear left to right. The upper images show typical morphologies observed by electron microscopy. Panels (a)–(c) have the same scale. Optical micrographs produced under crossed polarizers appear in the lower images [(d)–(f)] and all have the same scale. (a) Sample *A* (fluid phase): well-ordered lamellae (at the star) and few defects (arrows). (d) Sample *A*: vertical and horizontal oily streaks against a background devoid of defects. (b) Sample *B* (fluid-gel transition): curved regions of spherulite defects (arrow) interconnected by membranes (star). (e) Sample *B*: wispy lines as described in text. (c) Sample *C* (gel): smaller spherulites (arrow) and spherulites whose interior membranes are bent into crescents (stars). (f) Sample *C*: sheetlike texture (star) and extinction crosses (arrow).

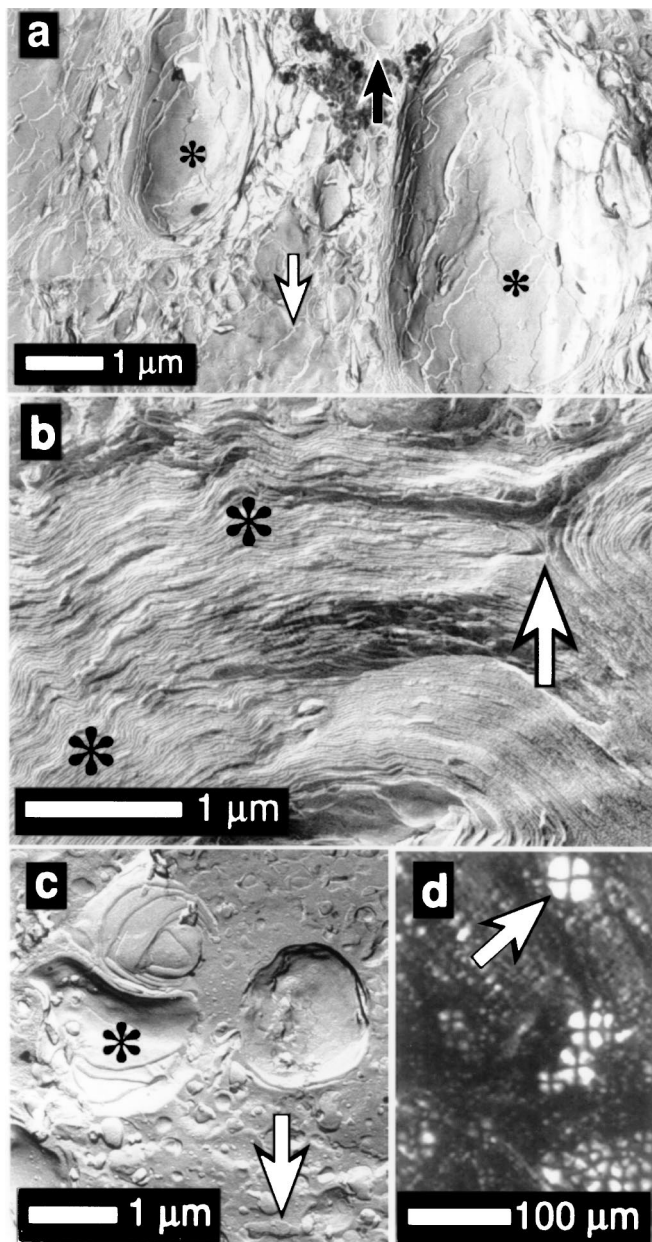


FIG. 3. (a),(b) Electron micrographs of gel sample C. (a) Large, aligned, anisotropic, cylinderlike spherulites (stars) among smaller spherulites (black arrow) and a network of connecting bilayers (white arrow). (b) Defects (at upper and lower edges) connected by undulating membranes (stars), some of which end in disclination-type defects (arrow). (c) Electron micrograph of multilamellar vesicles (MLVs) of DDAB which are not connected by membranes. Some vesicles are crescents (star) or elongated (arrow). (d) Optical micrograph (crossed polarizers) of DDAB MLVs with extinction crosses (arrow).

the *interconnections* between the spherulite defects give rise to an infinite network. Second, the random layer orientations inherently lead to elasticity because layers of membranes normal to the flow direction will resist shear [12]. Gelation is not due to entanglement of PEG. If this were true, the viscoelasticity would decrease with dilution instead of increasing. These electron microscopy observa-

tions are consistent with the model of Warriner *et al.* that the PEG-lipid diffuses in the plane of the membrane and segregates into curved regions stabilizing spherulite defects [5]. The micrographs of spherulites within a network of membranes are reminiscent of those seen in another swollen phase with low bending rigidity [13].

In polarized microscopy, the liquid phase (sample A, Fig. 1) exhibited “oily streaks” which were possible to anneal, characteristic of fluid bilayers [Fig. 2(d)] [11]. The background was black, indicative of oriented lamellae without defects. At the transition from the liquid to the gel phase (sample B, Fig. 1), wispy lines [Fig. 2(e)] and strings of very small ( $<10 \mu\text{m}$ ) extinction crosses appeared [Fig. 2(e), arrow]. Aligned, elongated spherulites would produce wispy lines. Alignment of interconnected spherulites may arise because the mixture is subjected to shear during preparation for polarized microscopy. In the gel phase (sample C, Fig. 1), the wispy texture became more uniform and sheetlike [Fig. 2(f), star], interspersed with extinction crosses [Fig. 2(f), arrow] produced by spherulites. The uniform gray background may have been due to unresolvable crosses. The defect structure in the gel (sample C) and in the transition sample (B) could not be annealed as in the liquid sample (A).

In previous work, x-ray diffraction determined that the lipid hydrocarbon chains were melted, and monitored the distance  $d$ , between membranes [5]. In the current work, the width of the first lamellar peak (001) was extracted. A wider peak indicates the average lamellar domain size was smaller. X-ray results confirm the electron microscopy conclusions: As the system becomes more viscous, there is an increase in defect density and a concomitant decrease in domain size. The (001) peak width increased from  $0.0034 \pm 0.0005 \text{ \AA}^{-1}$  (for sample A with  $d = 155 \pm 4 \text{ \AA}$ ) to  $0.0061 \pm 0.0005 \text{ \AA}^{-1}$  (for sample C with  $d = 188 \pm 6 \text{ \AA}$ ). The average lamellar domain was  $2200 \pm 200 \text{ \AA}$  for sample A and  $1000 \pm 200 \text{ \AA}$  for sample C [14].

To ascertain that the hydrogel was different from densely packed multilamellar vesicles [15], we prepared MLVs of dimethyldioctadecyl-ammonium bromium (DDAB, Avanti Polar Lipids, Alabaster, Alabama, purity of  $>99\%$ ) with 95% water [16]. By electron microscopy, a striking difference was the lack of membrane interconnections between spherulites in the onion phase [Fig. 3(c)]. Some anisotropic MLVs were found [Fig. 3(c), arrow], but never aligned as in the gel phase [Fig. 3(a)]. Crescent-shaped MLVs [Fig. 3(c), star] appeared similar to distorted spherulites in the gel phase [Fig. 2(c), stars]. By polarized microscopy, extinction crosses characteristic of spherulites were observed as expected [Fig. 3(d)] [15], but no wispy textures of the PEG-lipid hydrogel were observed. The cloudy background differed from the gel’s sheetlike texture; it was due to resolvable extinction crosses out of the focal plane.

At low-water content ( $\approx 60\%$ ), a liquid, low-viscosity phase existed at all concentrations of PEG lipid studied

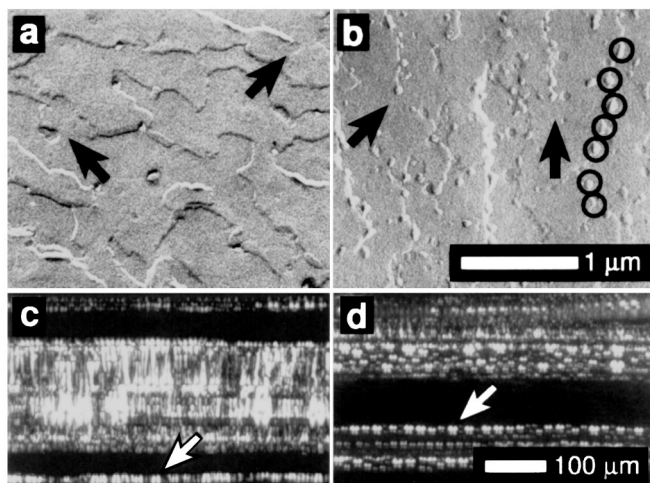


FIG. 4. Upper images are electron micrographs of samples *E* (a) and *F* (b) showing steps of flat lamellae interspersed with inclusions occasionally at screw dislocations (arrow). There was no obvious difference between the micrographs of samples *D* and *E* (not shown). Panels (a) and (b) have the same scale. In panel (b), inclusions preferentially decorate lamellar steps (circles). Lower images are optical micrographs (crossed polarizers) of sample *E* (c) and sample *F* (d) showing strings of extinction crosses (arrows) which can be annealed.

(black arrow in Fig. 1). Electron microscopy revealed planar lamellar sheets which could slide with low viscosity [Figs. 4(a) and 4(b)]. Large defects ( $\geq 1 \mu\text{m}$ ) with highly curved regions were rare. By polarized microscopy, few features were visible, consistent with electron microscopy observations. Before annealing, strings of extinction crosses followed the flow into the capillary during preparation [Figs. 4(c) and 4(d), arrows]. When annealed, the samples were black. No wispy or sheetlike textures of the gel phase appeared. By x-ray diffraction, the interlayer distance  $d$  was  $85\text{--}89 \text{ \AA}$  and the (001) peak width  $0.0023 \pm 0.0005 \text{ \AA}^{-1}$  [5]. Since this is smaller than peak widths of previous samples, the domain size of the low-water samples is larger, confirming electron microscopy observations.

By electron microscopy we discovered  $\sim 40 \text{ nm}$  bumps and divots in the membrane of the low-water samples. Their rounded shape implies that these features were inclusions in the membranes and not pores. The number of inclusions, but not their size, increased with the concentration of PEG lipid from sample *E* [Fig. 4(a)] to sample *F* [Fig. 4(b)], indicating they may be regions of higher PEG-lipid density. Inclusions often marked screw dislocations [Figs. 4(a) and 4(b), arrows]. In sample *F*, inclusions decorated the steps from one lamellar membrane layer to another [4(b), circles]. It is possible that the inclusions nucleated spherulite defects seen at higher water concentrations.

Freeze-fracture electron microscopy, polarized optical microscopy, and small-angle x-ray scattering show that the PEG-lipid hydrogel is characterized by a high defect density. Defects are connected by a network of bilayers

responsible for a high viscosity and elasticity. At low-water content, when the system is a low-viscosity liquid rather than a gel, we discover small ( $\sim 40 \text{ nm}$ ) inclusions in the membrane which can stabilize screw dislocations and may nucleate the hydrogel's defects.

J.A.Z. was supported by NSF Grant No. 9319447. C.R.S. and H.E.W. were partially supported by NSF Grant No. DMR9624091 and PRF Grant No. 31352-AC7. S.L.K. was supported by a UC President's Postdoctoral Fellowship. UCSB's Materials Research Laboratory is supported by NSF Grant No. DMR9632716.

\*Electronic address: slkeller@engineering.ucsb.edu

†Electronic address: heidi@mrl.ucsb.edu

‡Electronic address: safinya@engineering.ucsb.edu

§Electronic address: gorilla@squid.ucsb.edu

- [1] D. DeRossi *et al.*, *Polymer Gels: Fundamentals and Biomedical Applications* (Plenum, New York, 1991).
- [2] N. Peppas and R. Langer, *Science* **263**, 1715 (1994); V.H.L. Lee, *Peptide and Protein Drug Delivery* (M. Dekker, New York, 1991); F. Ilmain, T. Tanaka, and E. Kokufuta, *Nature (London)* **349**, 400 (1991); E. S. Matsu and T. Tanaka, *Nature (London)* **358**, 482 (1992); Y. Osada and S.B. Ross-Murphy, *Sci. Am.* **268**, 82 (1993).
- [3] A. Gabzion and D. Papahadjopoulos, *Proc. Natl. Acad. Sci. U.S.A.* **85**, 6949 (1988).
- [4] D.D. Lasic and F.J. Martin, *Stealth Liposomes* (CRC Press, Boca Raton, Florida, 1995).
- [5] H. Warriner, S.H.J. Idziak, N.L. Slack, P. Davidson, and C.R. Safinya, *Science* **271**, 969 (1996).
- [6] *The Physical Chemistry of Lipids*, edited by D.M. Small (Plenum, New York, 1986), Vol. 4.
- [7] C.R. Safinya, E.B. Sirota, D. Roux, and G.S. Smith, *Phys. Rev. Lett.* **62**, 1134 (1989).
- [8] S. Chiruvolu, E. Naranjo, and J.A. Zasadzinski in *Microstructure of Complex Fluids by Electron Microscopy*, edited by C.A. Herb and R.K. Prud'homme (American Chemical Society, Washington, D.C., 1994).
- [9] R. Fetter and M. Costello, *J. Microsc.* **141**, 277 (1986).
- [10] P. Boltenhagen, O.D. Lavrentovich, and M. Kleman, *Phys. Rev. A* **46**, R1743 (1992); M. Kleman, C.E. Williams, M.J. Costello, and T. Gulik-Krzywicki, *Philos. Mag.* **35**, 33 (1977).
- [11] G. Porte, J. Marignan, P. Bassereau, and R.J. May, *Europhys. Lett.* **7**, 713 (1988); N. Lei, C.R. Safinya, and R.F. Bruinsma, *J. Phys. II (France)* **5**, 1155 (1995).
- [12] K. Kawasaki and A. Onuki, *Phys. Rev. A* **42**, 3664 (1990).
- [13] P. Boltenhagen, M. Kleman, and O.D. Lavrentovich, *J. Phys. II (France)* **4**, 1439 (1994).
- [14] C.R. Safinya, D. Roux, G.S. Smith, S.K. Sinha, P. Dimon, N.A. Clark, and A.M. Belloq, *Phys. Rev. Lett.* **57**, 2718 (1986).
- [15] O. Diat and D. Roux, *J. Phys. II (France)* **3**, 9 (1993); H. Hoffmann, C. Thunig, P. Schmiedel, and U. Munkert, *Langmuir* **10**, 3972 (1994); P. Panizza, D. Roux, V. Vuillaume, C.Y. Lu, and M.E. Cates, *Langmuir* **12**, 248 (1996).
- [16] M. Dubois and T. Zemb, *Langmuir* **7**, 1352 (1991).